

Centrality of the collision and random matrix theory

Z. Wazir¹⁾

Department of Physics, COMSATS Institute of Information Technology, Islamabad, Pakistan

Abstract I discuss the results from a study of the central ^{12}C collisions at $4.2 A \text{ GeV}/c$. The data have been analyzed using a new method based on the Random Matrix Theory. The simulation data coming from the Ultra Relativistic Quantum Molecular Dynamics code were used in the analyses. I found that the behavior of the nearest neighbor spacing distribution for the protons, neutrons and neutral pions depends critically on the multiplicity of secondary particles for simulated data. I conclude that the obtained results offer the possibility of fixing the centrality using the critical values of the multiplicity.

Key words random matrix theory, UrQMD, central collisions, multiplicity

PACS 25.75.-q, 25.75.Dw, 25.75.Nq

1 Introduction

Centrality experiments are usually used to fix the baryon density of nuclear matter. These are considered to be the best tool to reach the Quark Gluon Phase (QGP) [1] of nuclear matter. Studying the different characteristics of events as a function of the centrality at JINR (Dubna), CERN (Geneva), BNL (New-York) and SIS (Darmstadt) could provide new information about the properties of nuclear matter under extreme conditions. On the other hand, the centrality of collisions cannot be defined directly in experiment. In different experiments, the centrality is defined [2–5] as the number of identified protons, projectile and target fragments, slow particles, charged particles as the energy flow of the particles with emission angles equal to 0° or 90° , etc. Apparently, it is not simple to compare quantitatively the results on centrality-dependences obtained in the literature, while on the other hand the definition of the centrality could significantly influence the final results. This may be why I could not get a clear signal on new phases of strongly interacting matter, though a lot of interesting information has been gathered from those experiments. From the last few years, some results from the central experiments are discussed which demonstrate the point of regime change and saturation on the behavior of some characteristics of the events as a function of the centrality [6]. It was

assumed that these phenomena could be connected with the fundamental properties of the strongly interacting matter and could reflect the changes of its states (phases) of strongly interacting matter.

2 UrQMD

The Ultra relativistic Quantum Molecular Dynamics (UrQMD) is a fully integrated Monte Carlo simulation package for proton+proton, proton+nucleus and nucleus+nucleus interactions. The UrQMD has many applications in particle physics, high energy experimental physics and engineering, shielding, detector design, cosmic ray studies and physics. The UrQMD [7–8] is a microscopic model based on a phase space description of nuclear reactions. The model was proposed mainly for a description of nucleus-nucleus interactions. It is the unique theoretical description of the underlying hadron-hadron interactions, with their vastly different characteristics at different incident energies and in different kinematic intervals. The UrQMD is appropriate for the description of the soft interactions because of the absence of the large Q^2 -scale. Therefore, low- p_T collisions are described in terms of the UrQMD model. The main goals of the code are to gain an understanding about the following physical phenomena within a single transport model.

1) Creation of dense hadronic matter at high tem-

Received 11 November 2009

1) E-mail: zafar_wazir@yahoo.com

©2010 Chinese Physical Society and the Institute of High Energy Physics of the Chinese Academy of Sciences and the Institute of Modern Physics of the Chinese Academy of Sciences and IOP Publishing Ltd

peratures.

2) Properties of nuclear matter, Delta and Resonance matter.

3) Creation of mesonic matter and of anti-matter.

4) Creation and transport of rare particles in hadronic matter.

5) Creation, modification and destruction of strangeness in matter.

6) Emission of electromagnetic probes.

The main ingredients of the model are the cross sections of binary reactions, the two-body potentials and decay widths of resonances [9–12]. In UrQMD, different fragmentation functions are used for leading nucleons and newly produced particles [13–15]. UrQMD is designed as a multipurpose tool for studying a wide variety of heavy ion related effects, ranging from multifragmentation and collective flow to particle production and correlations. Using UrQMD1.3 [7, 8], I generated 200000 events of ^{12}CC interaction at a momentum of 4.2 A GeV/ c in the lab frame.

3 Methodology

In this work, I used a method that does not depend on background information and relies only upon the fundamental symmetries of the composite system. Our approach is based on the Random Matrix Theory (RMT) [16], which was originally introduced to explain the statistical fluctuations of neutron resonances in compound nuclei [17]. Nowadays, RMT has become a standard tool for analysing the fluctuations in nuclei, quantum dots and many other systems [18]. The success of RMT is determined by the study of statistical laws governing the fluctuations having very different origins. Regarding the relativistic heavy ion collision data, the study of fluctuation properties of the momentum distribution of emitted particles could provide information about (i) possible errors in measurements and (ii) kinematical and dynamical correlations of the composite system.

Let us consider the discrete spectrum $\{E_i\}$, $i = 1, \dots, N$ of a d -dimensional quantum system (d is a number of degrees of freedom). A separation of fluctuations of a quantum spectrum can be based on the analysis of the density of states below some threshold E ,

$$S(E) = \sum_{i=1}^N \delta(E - E_i). \quad (1)$$

I can define a staircase function

$$N(E) = \int_{-\infty}^E S(E') dE' = \sum_{i=1}^N \theta(E - E'), \quad (2)$$

giving the number of points on the energy axis which

are below or equal to E . Here,

$$\theta(x) = \begin{cases} 0, & \text{for } x < 0 \\ 1, & \text{for } x > 0 \end{cases}. \quad (3)$$

I separate $N(E)$ in a smooth part $\zeta(E)$ and the remainder that will define the fluctuating part $N_{\text{fl}}(E)$,

$$N(E) = \zeta(E) + N_{\text{fl}}(E). \quad (4)$$

The smooth part $\zeta(E)$ can be determined either from semi classical arguments or using a polynomial or spline interpolation for the staircase function. To study the fluctuations, I have to get rid of the smooth part. The usual procedure is to “unfold” the original spectrum $\{E_i\}$ through the mapping $E \rightarrow x$,

$$x_i = \zeta(E_i), \quad i = 1, \dots, N. \quad (5)$$

Now I can define spacing s_i (the same for all) $= x_{i+1} - x_i$ between two adjacent points and collect them in a histogram. The effect of mapping is that the sequence $\{x_i\}$ has on the average a constant mean spacing (or a constant density), irrespective of the particular form of the function $\zeta(E)$ [19]. To characterize the fluctuations, one deals with different correlation functions [20]. In this paper, I will use only a correlation function related to the spacing distribution between adjacent levels. Below, I follow a simple heuristic argument due to Wigner [21] that illustrates the presence or absence of level repulsion in an energy spectrum.

For a random sequence, the probability that the level will be in the small interval $[x_0 + s, x_0 + s + ds]$ is independent of whether or not there is a level at x_0 . Given a level at x_0 , let the probability that the next level be in $[x_0 + s, x_0 + s + ds]$ be $p(s) ds$. Then for $p(s)$, the nearest-neighbor spacing distribution, I have

$$p(s) ds = p(1 \in ds | 0 \in s) p(0 \in s). \quad (6)$$

Here, $p(n \in s)$ is a probability that the interval of length s contains n levels and $p(n \in ds | m \in s)$ is the conditional probability that the interval of length ds contains n levels, when that of length s contains m levels. One has $p(0 \in s) = \int_s^\infty p(s') ds'$, the probability that the spacing is larger than s . The term $p(1 \in ds | 0 \in s) = \mu(s) ds$ [$\mu(s)$ is the density of spacings s], depends explicitly on the choices, 1 and 0, of the discrete variables n, m . As a result, one obtains $p(s) = \mu(s) \int_s^\infty p(s') ds'$ which can be solved to give

$$p(s) = \mu(s) \exp\left(-\int_0^s \mu(s') ds'\right). \quad (7)$$

The function $p(s)$ and its first moment are normalized

to unity,

$$\int_0^\infty p(s)ds = 1, \quad \int_0^\infty sp(s)ds = 1. \quad (8)$$

For a linear repulsion $\mu(s) = \pi s/2$, one obtains the Wigner surmise,

$$p(s) = \frac{\pi}{2}s \exp\left(-\frac{\pi}{4}s^2\right), \quad s \geq 0. \quad (9)$$

For a constant value $\mu(s)=1$, one obtains the Poisson distribution

$$p(s) = \exp^{-s}, \quad s \geq 0. \quad (10)$$

As discussed above, when the quantum numbers of levels are well defined, one should expect for the spacings the Poisson type distribution, while a Wigner type distribution occurs due to either internal or external perturbations that destroy these quantum numbers. In fact, one of the sources of external perturbations can be attributed to the uncertainty in the determination of the momentum distribution of emitted particles in relativistic heavy ion collisions. I make a conjecture that the above discussed ideas of

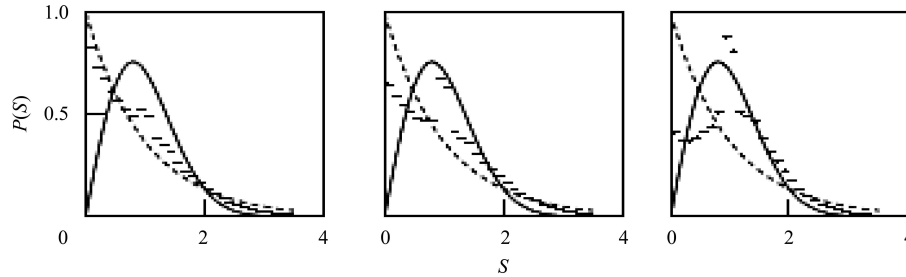


Fig. 1. Using the UrQMD data for all nucleons (n, p), the nearest neighbor spacing momentum distribution $P(S)$ for different regions of measured momenta: the first column corresponds to $0.1 < |p| < 1.14$ GeV/c; the second column corresponds to $1.14 < |p| < 4.0$ GeV/c; and the third column corresponds to $4.0 < |p| < 7.5$ GeV/c. The Poisson and the Wigner surmise distributions are connected by the dashed and solid lines, respectively.

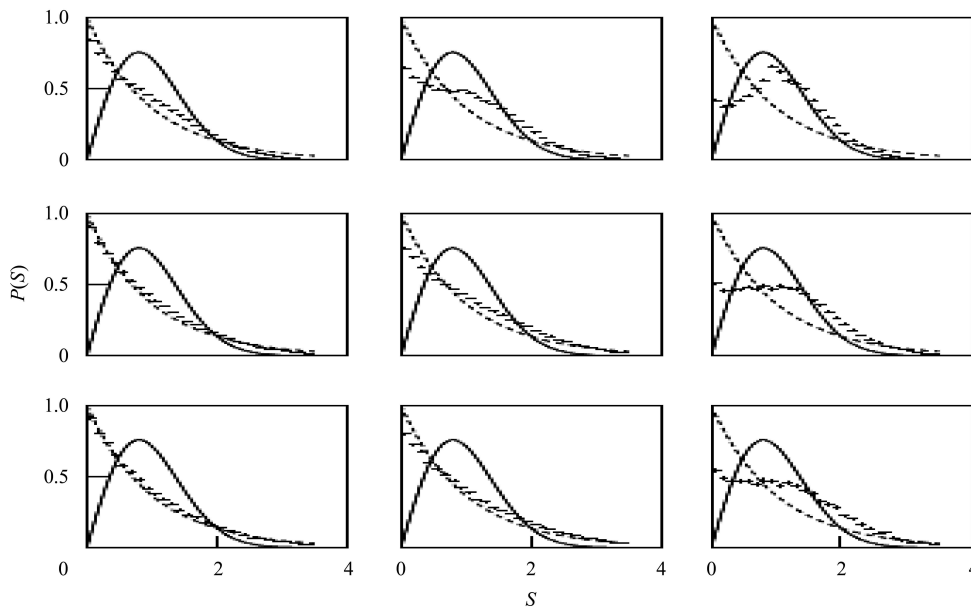


Fig. 2. Using the UrQMD data for nucleons (n, p)=10–14, 15–19, 20–24, the nearest neighbor spacing momentum distribution $P(S)$ for different regions of measured momenta: the first column corresponds to $0.1 < |p| < 1.14$ GeV/c; the second column corresponds to $1.14 < |p| < 4.0$ GeV/c; and the third column corresponds to $4.0 < |p| < 7.5$ GeV/c. The Poisson and the Wigner surmise distributions are connected by the dashed and solid lines, respectively.

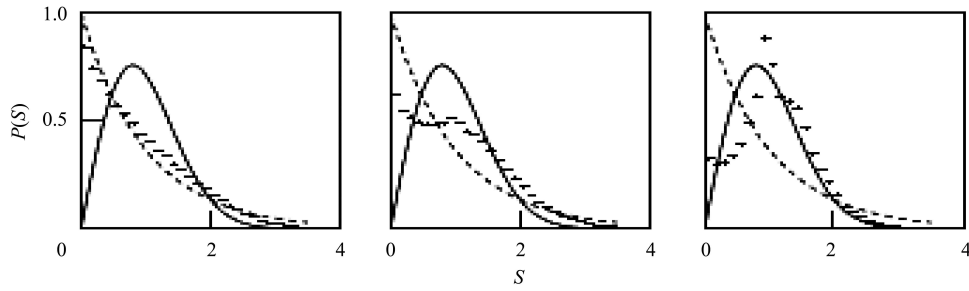


Fig. 3. Using the UrQMD data for all neutral particles (n , π^0), the nearest neighbor spacing momentum distribution $P(S)$ for different regions of measured momenta: the first column corresponds to $0.1 < |p| < 1.14$ GeV/c; the second column corresponds to $1.14 < |p| < 4.0$ GeV/c; and the third column corresponds to $4.0 < |p| < 7.5$ GeV/c. The Poisson and the Wigner surmise distributions are connected by the dashed and solid lines, respectively.

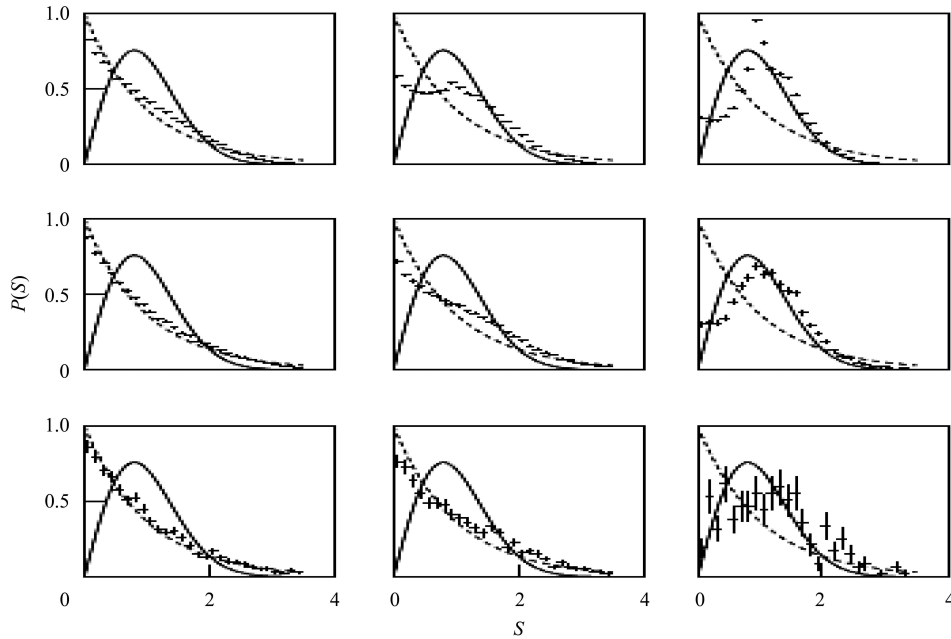


Fig. 4. Using the UrQMD data for neutral particles (n , π^0)=10–14, 15–19, 20–22, the nearest neighbor spacing momentum distribution $P(S)$ for different regions of measured momenta: the first column corresponds to $0.1 < |p| < 1.14$ GeV/c; the second column corresponds to $1.14 < |p| < 4.0$ GeV/c; and the third column corresponds to $4.0 < |p| < 7.5$ GeV/c. The Poisson and the Wigner surmise distributions are connected by the dashed and solid lines, respectively.

the RMT are applicable to the momentum distribution. Therefore, I simply replace in Eqs. (1)–(5) the variable E with the variable P and construct the corresponding correlation function $P(S)$.

To identify the correlations between nucleons and neutral particles, I divided the set of spacings $\{s_i\}$ into three sets, in correspondence with three regions of the measured momenta: a) $0.1 < |p| < 1.14$ GeV/c (Region I); b) $1.14 < |p| < 4.0$ GeV/c (Region II); and c) $4.0 < |p| < 7.5$ GeV/c (Region III) (see Figs. 1–4).

4 Results and discussion

I can see the distributions of $p(s)$ functions for all nucleons (n , p) and for all neutral particles (n , π^0) in the three regions of momentum from the UrQMD data, as shown in Figs. 1 and 3. I can see the Poisson distribution in Region I, while Wigner distribution is in Region III. These results show the existence of some peaks in the region of II and their transformation to the Wigner distribution in the region of III. These results demonstrate the existence of some non-

trivial non-kinematic correlations for the secondary nucleons and neutral particles in the regions of II and III.

To observe the changes with multiplicity, I divide the events in the three groups from UrQMD data for nucleons (n, p): i) the events with $N=10-14$; ii) the events with $N=15-19$; and iii) the events with $N=20-24$ and for neutral particles (n, π^0): i) the events with $N=10-14$; ii) the events with $N=15-19$; and iii) the events with $N=20-22$.

I can see from Figs. 2 and 4 that the correlation between secondary nucleons and neutral particles decreases inversely with the multiplicity of secondary nucleons and neutral particles.

I can see the Poisson distribution in Region I, but the behavior of $P(S)$ functions changes inversely with the multiplicity for Region II and III for nucleons and neutral particles. The Wigner type behavior disappears (or becomes weaker essentially) in Region III with the increasing number of nucleons and

neutral particles. So the results from Figs. 2 and 4 demonstrate uniquely that the observed structure for the $P(S)$ behaviors for nucleons and neutral particles with the momentum in II and III ranges is connected with the multiplicity. At high multiplicity I could see that the correlation which was the reason for non-Poisson behavior of $p(s)$ function for nucleons and neutral particles with greater momentum decreases.

5 Conclusion

In conclusion, one can say that the simulated data coming from the UrQMD code show the critical change in the behavior for the nearest neighbor spacing momentum distribution for protons, neutrons and neutral pions produced in ^{12}CC -reactions at $4.2 \text{ A GeV}/c$ with multiplicity. So I could conclude that the obtained results offer the possibility of fixing the centrality using the critical values of the multiplicity.

References

- 1 Collins J C, Perry M J. Phys. Rev. Lett., 1975, **34**: 1353
- 2 Kotuku A P, Gorenstein M I, Stöcker H, Greiner W. Phys. Rev. C, 2003, **68**: 041902
- 3 Suleymanov M K et al. 2007. ArXiv:0712.0062v1 [nucl-ex]
- 4 Mohanty B et al. Phys. Rev. C, 2003, **68**: 021901
- 5 Suleimanov M K et al. Phys. Rev. C, 1998, **58**: 351
- 6 Suleymanov M K et al. Nuclear Physics B (Proc. Suppl.), 2008, 177-178: 341
- 7 Bass S A et al. Prog. Part. Nucl. Phys, 1998, **41**: 225
- 8 Bleicher M et al. J. Phys. G, 1999, **25**: 1859
- 9 Aichelin J. Phys. Rept., 1991, **202**: 233
- 10 Aichelin J, Rosenhauer A, Peilert G, Stocker H, Greiner W. Phys. Rev. Lett., 1987, **58**: 1926
- 11 Aichelin J, Stocker H. Phys. Lett., B, 1986, **176**: 14
- 12 Peilert G et al. Phys. Rev. C, 1989, **39**: 1402
- 13 Andersson Bo, Gustafson G, Soderberg B. Z. Phys. C, 1983, **20**: 317
- 14 Field R D, Feynman R P. Phys. Rev. D, 1977, **15**: 2590
- 15 Field R D, Feynman R P. Nucl. Phys. B, 1978, **136**: 1
- 16 Mehta M L. Random Matrices Second ed. Academic, New York: 1991
- 17 Porter C E. Statistical Theories of Spectra: Fluctuations, Academic, New York: 1965
- 18 Cuhf T, Muller-Groeling A, Weidenmüller H. Phys. Rep., 1998, **299**: 189
- 19 Bohigas O. Lecture Notes in Physics, 1986, **263**: 18 (Springer-Verlag)
- 20 Mehta M L. Random Matrices Second ed. Academic, New York: 1991
- 21 Wigner E P. Contribution to Conference on Neutron Physics by Time-of-Flight. Gatlinburg, Tennessee: 1956